NONLINEAR TRANSPORT IN BALLISTIC SEMICONDUCTOR DIODES WITH NEGATIVE EFFECTIVE MASS CARRIERS

B. R. Perkins, Jun Liu, and A. Zaslavsky,
Div. of Engineering Brown University Providence, RI 02912, U.S.A.,

Z. S. Gribnikov and V. V. Mitin,
Dept. of Electrical and Computer Engineering,
Wayne State Univ. Detroit, MI 48202, U.S.A.

E. P. De Poortere, M. Shayegan,
Dept. of Electrical Engineering,
Princeton University, Princeton, NJ 08544, U. S. A.

We are pursuing a new class of solid-state devices capable of generating high-frequency radiation: short ballistic semiconductor diodes in which the current flow is due to carriers injected into a negative-effective-mass (NEM) region of dispersion [1]. The resulting radiation is tunable by the source-drain voltage applied to the diode and device operation does not require magnetic fields or pumping by other oscillators. The physical mechanism responsible for high-frequency oscillation generation in such diodes lies in the instability of the ballistic NEM carrier quasineutral plasma, which forms in a large fraction of the diode base and stratifies into accumulation and depletion domains. As in the Gunn diode, where the instability arises from intervalley carrier transfer, the domains travel from source to drain and give rise to current oscillations. However, in short ballistic diodes the source-drain distance L can be much smaller than in a Gunn diode; numerical simulations show that for $L \leq 0.2$ μm the ballistic transport of the domains can lead to current oscillations in the THz frequency range [2].

The implementation of such ballistic diodes requires two essential ingredients. First, the current carriers should have an accessible NEM region in their dispersion. Second, the carriers must have a long mean-free-path and the diode a sufficiently short source-drain separation L for the majority of the carriers to remain ballistic. The most technologically mature semiconductor system with

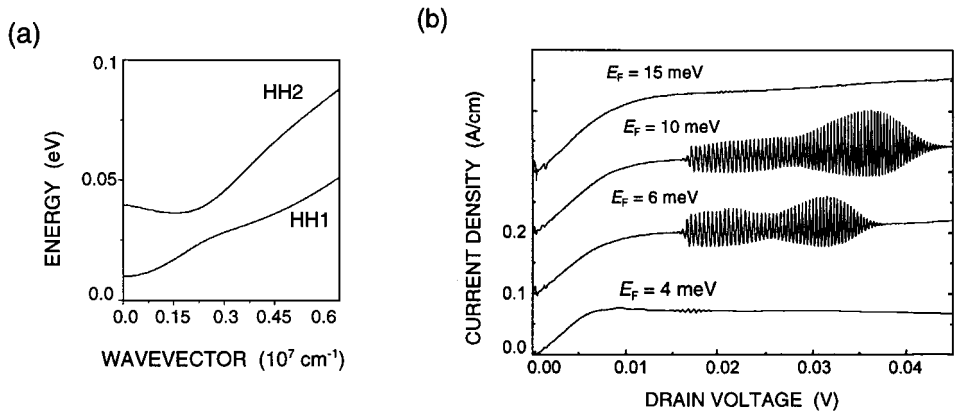

Figure 1: (a) The in-plane dispersion of the two lowest quantized hole subbands in a GaAs/AlAs quantum well of 8 nm width. The lowest subband exhibits NEM. (b) Simulated current-voltage characteristics with oscillations for different Fermi energies of holes entering the base (source-drain distance L = 0.1 μm). The voltage sweep rate in the simulation is 0.5 mV/ps.

the required dispersion consists of narrow p-GaAs quantum wells (QWs), where the degeneracy of the heavy and light hole branches of the dispersion is lifted by size quantization and the required NEM section appears in the in-plane dispersion due to anti-crossing behavior of the hole subbands. A narrow $\sim$7-8 nm GaAs QW confined by AlAs barriers places the NEM section some 20 meV above the bottom of the lowest subband, as shown in Fig. 1(a). This eliminates optical phonon scattering, the dominant mechanism limiting carrier mean-free-path at low temperatures, because the LO-phonon energy in GaAs is 36 meV. Further, by growing the GaAs/AlGaAs heterostructure on a $<311>$A GaAs substrate, one can achieve an exceptionally high hole mobility. In modulation-doped $<311>$A GaAs/AlGaAs heterostructures, mean-free-paths $\lambda \gg 1$ μm at low temperature have been reported [3],[4].

Simulated current-voltage characteristics of short p-GaAs QW ballistic diodes with in-plane dispersion of Fig. 1(a) and hole densities in the 10^{11} cm^{-2} range are shown in Fig. 1(b). These simulations, which assume fully ballistic transport and solve the nonstationary ballistic equations self-consistently with the two-dimensional Poisson equation inside and outside the QW, predict quasiperiodic oscillations for relatively small drain voltages $V \sim 20-30$ mV, with maximum oscillation frequency above 1 THz [2].

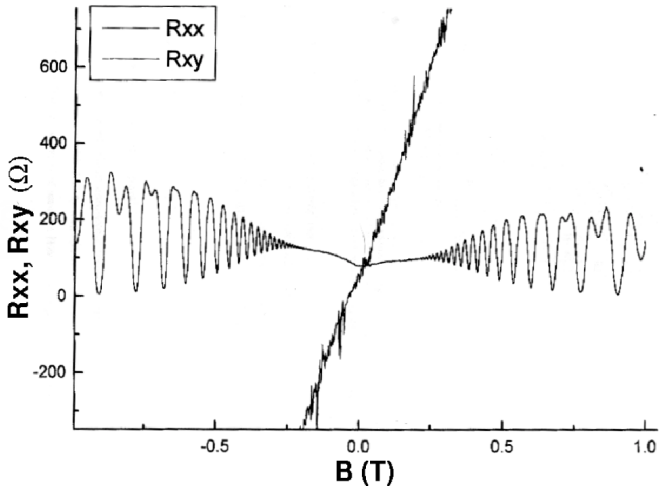

Figure 2: Magnetoresistance data for 2D hole gas in our narrow p-GaAs QW modulation-doped heterostructure (well width $\sim$7 nm) at T = 4.2 K. The Shubnikov-de Haas oscillations are characteristic of hole mobility $\sim$50,000 cm^2/V$\cdot$s.

The initial material for our diodes was narrow p-GaAs QW modulation-doped heterostructure grown on a <311>A substrate, characterized by magnetoresistance measurements on large Van der Pauw geometry samples at T = 4.2 K shown in Fig. 2. The hole density in the $\sim$7 nm QW is $\sim$2.5x10^{11} cm^{-2}, while the low-field mobility is $\sim$50,000 cm^2/V$\cdot$s. When a two-terminal diode is fabricated from this material, the current-voltage $I(V)$ characteristics depend on the source-drain separation L. When L is large, say L = 1 μm, the transport is non-ballistic. At very low V the diode $I(V)$ should be Ohmic, with the resistance determined by the density and mobility μ of the 2D hole gas in the QW. At higher V, corresponding to a 0.01$-$0.05 V drop over the base, the $I(V)$ is non-Ohmic even in the absence of ballistic transport, either due to the heating of holes in high electric fields (10^2-10^3 V/cm) or due to the space-charge-limited injection of holes from the p^+ source contact. However, once L becomes smaller than the carrier mean-free-path, the $I(V)$ characteristics can be shown to follow a $V^{1/2}$ dependence as long as the hole dispersion is parabolic. The existence of a NEM section in the dispersion alters the $I \sim V^{1/2}$ dependence as shown in Fig. 1(b) because the homogeneous distribution of carriers accelerated to the NEM section is convectively

unstable [1]. The convective instability becomes global, leading to current oscillations (plotted in Fig. 1(b) as a function of the Fermi energy E_F in the p^+ injecting contact). These oscillations, in turn, transform such diodes into generators of high-frequency radiation. While the high-frequency oscillations are unobservable in dc measurements, simulations [2] predict that the dc $I(V)$ current will saturate at a source-drain V sufficient to accelerate a large fraction of the ballistic carriers to the NEM region of the dispersion.

The submicron diodes were fabricated and integrated with an on-chip wideband spiral antenna for coupling out the high-frequency radiation using a two-step lithographic and metal lift-off process illustrated in Fig. 3. First, electron-beam lithography is used to define the initial source and drain contacts. A source drain distance of as low as 0.2 μm is readily achievable. For Ohmic contacts Au/Zn/Au metallization was used, with a thin (5 nm) bottom layer of Au for adhesion, a $10-20$ nm layer of Zn for the actual p-type contact, and a final thick (50-100 nm) layer of Au to encapsulate the volatile Zn [6]. These contacts are subsequently annealed at $500-600$ °C for $2-5$ minutes. Recently, in order to lower the contact resistance, we began investigating alternative contact metallization schemes, based on the W/Zn/W recipe developed for p-HEMTs [7]. In either case, once the source and drain contacts are annealed, photolithography is used to define the wideband antenna spiral contacts, shown in Fig. 3, using a lift-off process with Ti/Au metallization. The devices are finally bonded and measured in a variable temperature insert (T controllable from 1.6 K to room temperature) of an Oxford Instruments magnetocryostat.

Figure 4(a) shows the measured $I(V)$ characteristics at T = 1.7 K in a diode with metallurgical L = 0.5 μm with and without a magnetic field B normal to the plane of the QW (note that the actual source-drain separation L_{eff} is smaller than 0.5 μm due to sideways diffusion of the contact metal). The $I(V,B{=}0)$ lineshape exhibits the saturation predicted by the transport simulations of Fig. 1(b) near to the predicted current density of $\sim$0.1 A/cm but in a much higher range of drain voltage. This indicates considerable series resistance in the contacts. In fact, by comparing the measured resistance near V = 0 with what can be expected from the density and mobility of the hole gas in the QW, one arrives at an estimated series resistance in the contacts on the order of 1kΩ. Figure 4(b) shows the same data corrected for a contact series resistance of 800 Ω, which brings the B = 0 resistance at low V into agreement with the hole gas density and mobility. The voltage needed for current saturation then falls below 50 mV, as predicted by Fig. 1(b).

As can be seen in Figs. 4(a) and (b), the magnetic field B suppresses the

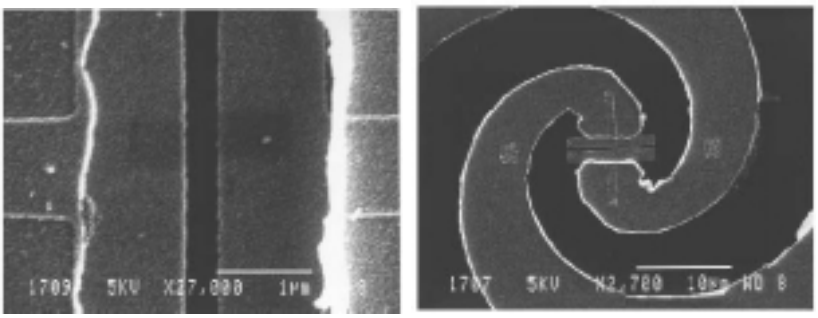

Figure 3: Scanning electron micrograph of the source-drain gap of a ballistic diode fabricated by e-beam lithography, with a metallurgical source-drain distance $L \sim$ 0.3 μm and Au/Zn/Au contact metallization (left) and the integration of the diode with a wideband spiral antenna defined by optical lithography (right). The width of the source and drain contacts is $\sim$ 10 μm.

current I. This suppression is strongest at low V and then the $I(V)$ slope begins to increase, as can be seen more clearly in the conductance dI/dV that is also shown. A rough quantitative picture of the expected $I(V)$ characteristics in our diodes in a normal B field can be obtained by assuming the drain current I can be separated into ballistic and diffusive components that can be treated separately. To first order, a small B has little effect on the diffusive component, while the ballistic carriers are deflected and follow a cycloid. At a given magnetic field, there is a critical source drain voltage below which ballistic current cannot reach the drain. This critical voltage V_c has the value:

$$V_c(B) = \frac{eB^2L^2}{2m^*} \tag{1}$$

which increases quadratically with B and L. The magnitude of the ballistic current density in the presence of B can be described for $V > V_c(B)$ by:

$$J = en_0\sqrt{\frac{e}{2m^*}(V - \frac{eB^2L^2}{2m^*})}(1 + \frac{\epsilon B^2}{m^*n_0}) \tag{2}$$

where n_0 is the 2D hole density, m^* is the effective mass, and ϵ is the dielectric constant.

The resulting $I(V)$ characteristic is schematically shown in Fig. 5 for B = 0, in which case the total current consists of a linear diffusive component and a saturating ballistic component, and for two magnetic fields $B_1 < B_2$, which suppress

(a)

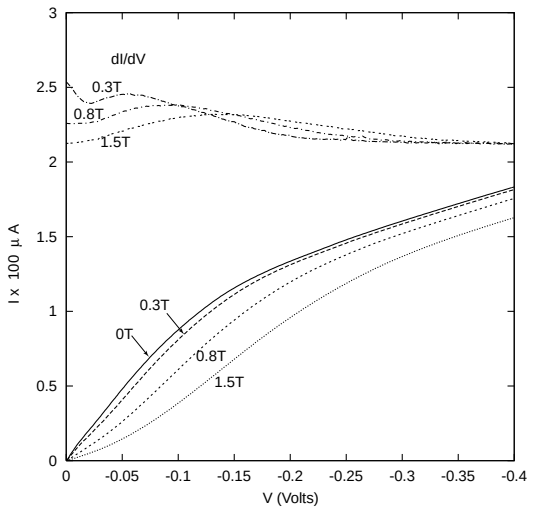

(b)

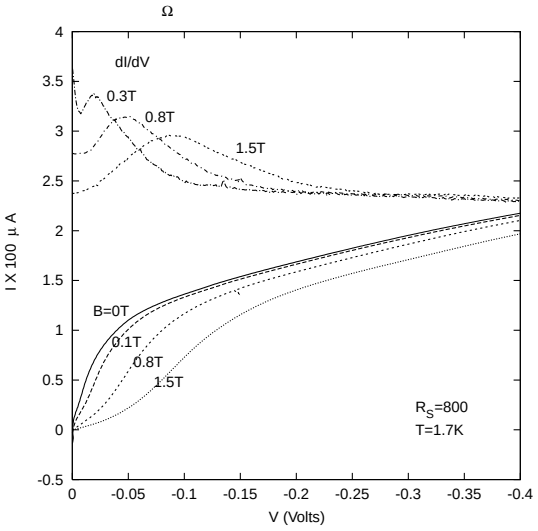

Figure 4: (a) Measured low-temperature $I(V)$ characteristics for B = 0, 0.3, 0.8 and 1.5 T at T = 1.7 K (a) of a planar ballistic diode (metallurgical source-drain separation L = 0.5 μm, source and drain contact width = 10 μm). (b) The same data corrected for a series resistance R_S = 800 Ω in the contacts. The strong current saturation for $V < 50$ mV and the quenching of the $I(V)$ by a small magnetic field are consistent with ballistic transport.

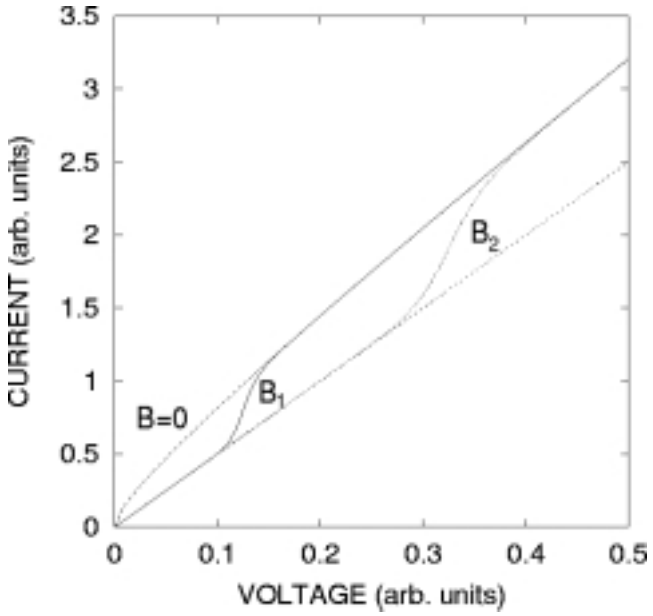

Figure 5: Schematic theoretical $I(V)$ curve of a short diode in a small magnetic field B. The current is assumed to consist of two components: diffusive that is largely unaffected by B (dashed line) and ballistic that is predicted to saturate following a roughly $V^{1/2}$ dependence, as in Fig. 1(b). In a B field, the total current is partially suppressed up to the critical field V_c and then rejoins the B = 0 curve, as shown for two arbitrary B field values, with $B_1 < B_2$.

the current up to the critical drain voltage $V_c(B)$. Of course, the approximation in which these two current components are simply summed is quite crude: in reality, the existence of a diffusive component disrupts the electric field field distribution in the base used to derive Eq. (2). This, together with the large series resistance in the contacts and the weaker saturation of the source-drain current than predicted by the fully ballistic models [2] makes quantitative comparison with experimental data premature. However, a comparison of the $I(V,B)$ data corrected for series resistance shown in Fig. 4(b) with Fig. 5 indicates that the measured $I(V)$ characteristics are consistent with partially ballistic hole transport between source and drain.

We should note that another possible source of the excessively high source-drain resistance in our diodes, in addition to high-resistance contacts, is the escape of hot holes from the QW channel into the acceptor-doped AlGaAs regions that supplied the 2D hole density in the first place. This is the well-known real-space

transfer effect that can occur in heterostructures during in-plane transport [8]. If, after improving the source-drain contacts, we find that real-space transfer affects our $I(V)$ characteristics by significantly reducing the density of holes in the QW, we may need to redesign the modulation-doping scheme by increasing the Al content in the doped regions.

Encouraged by the measured nonlinearities in the $I(V)$ curves of our short diodes made from p-GaAs QW heterostructures with high mobilities and in-plane NEM dispersion, we are continuing to work on improved contacting techniques. When more reliable fabrication technology is available, the devices will be tested for high-frequency radiation. We anticipate that such ballistic diodes, together with related three-terminal devices produced by gating this material in a field-effect transistor geometry [5], will offer an alternative route towards solid-state THz local oscillators for astrophysics applications.

References

[1] Z. S. Gribnikov and A. N. Korshak, *Semiconductors* **28**, 812 (1994).

[2] Z. S. Gribnikov, A. N. Korshak, and V. V. Mitin, *Intern. J. Infrared Millimeter Waves* **73**, 213 (1999) and references therein.

[3] J. J. Heremans, M. B. Santos, K. Hirakawa, and M. Shayegan, *J. Appl. Phys.* **76**, 1980 (1994).

[4] M. Henini, R. J. Rodgers, P. A. Crump, B. L. Gallagher, and G. Hill, *Appl. Phys. Lett.* **65**, 2054 (1994).

[5] A. N. Korshak, Z. S. Gribnikov, N. Z. Vagidov, and V. V. Mitin, *Appl. Phys. Lett.* **75**, 2292 (1999).

[6] P. J. Rogers, C. J. G. M. Langerak, B. L. Gallagher, R. J. Barraclogh, M. Henini, T. J. Foster, G. Hill, S. A. J. Wiegers and J. A. A. J. Perenboom *Physica B* **184**, 95 (1993).

[7] S. Tiwari, J. Hintzman, and A. Callegari, *Appl. Phys. Lett.* **51**, 2118 (1987).

[8] Z. S. Gribnikov, K. Hess, and G. Kosinovsky, *J. Appl. Phys.* **77**, 1337 (1995).